Int. J. Electrochem. Sci., 14 **(2019)** 8506 – 8513, doi: 10.20964/2019.09.04

International Journal of ELECTROCHEMICAL SCIENCE
www.electrochemsci.org

Short Communication

An Intelligent Corrosion Inhibitor Based on pH-sensitive poly(2-diethylaminoethyl methacrylate) Microspheres

Yuwan Tian[1,2], Cheng Wen[1,2,], Chaofang Dong[2], Gui Wang[3], Peichang Deng[3], Guanting Zhou[3]*

[1] School of Mechanical and Power Engineering, Guangdong Ocean University, Zhanjiang 524088, China
[2] Corrosion and Protection Center, Institute for Advanced Materials and Technology, University of Science and Technology Beijing, Beijing 100083, China
[3] Guangdong Technology Center of Marine Equipment and Manufacture, Guangdong Ocean University, Zhanjiang 524088, China
[*]E-mail: wcheng.3jia@163.com

Received: 9 April 2019 / *Accepted:* 19 June 2019 / *Published:* 31 July 2019

A low pH-triggered intelligent corrosion inhibitor based on BTA loaded poly(2-diethylaminoethyl methacrylate) (PDEAEMA) microspheres was designed to prevent metal corrosion in a variable pH environment. The average particle size of the microspheres was 3 μm. The microspheres swelled at low pH values and shrank at high pH values, which guarantees pH sensitivity. The BTA release from the intelligent corrosion inhibitor depends on the environment pH value. The electrochemical results revealed that the intelligent corrosion inhibitor exhibited smart and efficient corrosion inhibition performance on steel corrosion, which was attributed to the pH-dependent supply of BTA.

Keywords: intelligent, pH-sensitive, microsphere, inhibit

1. INTRODUCTION

Corrosion is a spontaneous phenomenon in both natural and industrial environments that always limits the performance and service life of metal structures. Globally, the cost of corrosion is more than US $4 trillion a year. The prevention and control of corrosion accounts for half of these costs, while damages and lost productivity account for the rest [1].

The application of corrosion inhibitors is one of the most common and cost-effective methods to promote corrosion resistance. Inhibitors have been used in various conditions without the need for special equipment, and they have no negative effect on the original properties of the materials. BTA and its derivatives are among the most effective organic inhibitors [2]. Yao reported that the adsorption of BTA on steel was the main inhibition mechanism, and each iron atom could coordinate with several BTA ions [3]. The complex layer of [$Fe_nCl_pBTA_m$] acts as a barrier to restrict the dissolution of steel

[4]. However, when directly used, BTA is susceptible to decomposition over time, resulting in the waste of resources and premature inactivation.

Intelligent corrosion inhibitors have been developed to overcome these problems. They are made of a conventional corrosion inhibitor as the core and a sensitive carrier as the shell. The shell appropriately responds to external stimuli (such as pH [5–7], ions [8–10], redox reactions [11], and lasers [12]). As a result, the core has a controlled and sustained release from the intelligent corrosion inhibitor. Generally, metal shows more corrosion at low pH (acidic conditions), and thus, intelligent corrosion inhibitors exhibiting low pH-triggered corrosion protection in a variable pH environment can find wide applications in civil engineering. Such intelligent corrosion inhibitors are developed based on pH-responsive hydrogel discs prepared via photocrosslinking, thermal polymerization, or radiation polymerization. Presently, numerous intelligent corrosion inhibitors based on polyelectrolytes are available. However, intelligent corrosion inhibitors need to be incorporated into micro/nanoparticles for the better adaption to environmental conditions. The preparation of microspheres generally comprises emulsions [13], interfacial polymerization [14], organically modified mesoporous materials [15], and coprecipitation methods [16]. Among them, emulsions can be divided into polymer entanglements of long chains and the polymerization of small molecule monomers.

Here, we report the synthesis and inhibition efficiency of a new intelligent corrosion inhibitor exhibiting low pH-triggered corrosion protection. The new inhibitor was prepared using oil-in-water emulsion synthetic PDEAEMA microspheres as the microcarrier. BTA was loaded into the PDEAEMA microspheres. The BTA release behavior was studied at different pH values. The effect of the intelligent corrosion inhibitor on steel corrosion in an acidic NaCl solution after immersion for 6 h was evaluated by electrochemical impedance spectroscopy and polarization curves.

2. MATERIALS AND METHODS

2.1 Preparation of the intelligent corrosion inhibitor

The pH-sensitive PDEAEMA microspheres were synthesized by a three-step oil–water emulsification method. Firstly, an aqueous solution (50 mL) of sodium dodecyl sulfate (SDS) (25 g/L) was slowly added to a mixed oily solution (10 mL) of a 2-(Diethylamino) ethyl methacrylate (DEAEMA) monomer (461 g/L), an Ethylene Glycol Dimethyl Acrylate (EGDMA) crosslinker (66 g/L), and an azodiisobutyronitrile (AIBN) initiator (5 g/L). Then, the oil–water emulsion was mixed with an ultrasonic cell disrupter for 5 min to obtain a stable Pickering emulsion. Finally, the resulting PDEAEMA microspheres were removed from the Pickering emulsion after stirring at 1000 rpm and 65 °C for 7 h.

BTA was loaded into the PDEAEMA microspheres to obtain the intelligent corrosion inhibitor. The PDEAEMA microspheres (0.6 g) were added to a continuously stirred BTA-ethanol solution (100 mL, 1 g/L) at room temperature for 24 h. Then, the precipitates were collected, washed, and dried under vacuum. The amount of entrapped BTA in the intelligent corrosion inhibitor was calculated as the concentration difference between the initial and final BTA-ethanol solution.

All chemical reagents were of analytical grade purchased from Aladdin (Shanghai, China). All reagents were directly used without further purification.

2.2 Release behavior of the intelligent inhibitor

The intelligent corrosion inhibitor (5 mg) was submerged in buffer solution (80 mL) at pH 2.0, 6.0, and 9.0, respectively. The suspensions were then magnetically stirred continuously for 24 h. The amount of released BTA was measured using a HITACHI U3900H UV-Vis spectrophotometer at predetermined time intervals.

2.3 Inhibition efficiency of the intelligent inhibitor

Carbon steel (0.19% C, 0.57% Si, 0.57% Mn, 0.024% S, 0.017% P) was used to study the protective effect of the intelligent corrosion inhibitor. The corrosion behaviors of carbon steel in the acidic solutions were studied by electrochemical impedance spectra (EIS) and polarization curves using a PARSTAT 2273 electrochemical station. The electrolytes were 0.1 M NaCl at pH 6.0 without BTA, with 25 mg/L BTA, and with an equivalent amount of intelligent corrosion inhibitor. To evaluate the long-term efficiency, the working electrodes were immersed in the electrolyte for 6 h before electrochemical testing. A three-electrode system comprising a saturated calomel electrode (SCE) as the reference electrode, a platinum sheet as the counter electrode, and a carbon steel as the working electrode was used. The EIS spectra were obtained by frequency sweep from 100 kHz to 10 mHz at open circuit potential with 10 mV AC perturbation. The polarization curves were measured at a scan rate of 0.1 mV/s.

3. RESULTS AND DISCUSSION

3.1 Fabrication of the intelligent inhibitor

The procedure for fabricating the intelligent inhibitor is shown in Fig. 1. The crosslinked three-dimensional net structure of the PDEAEMA polymer was formed in the presence of the EGDMA crosslinker. The mean size of the PDEAEMA microspheres was approximately 3 μm, as shown in Fig. 2. The BTA corrosion inhibitor adsorbed to the interface of the PDEAEMA microspheres because of the three-dimensional net structure.

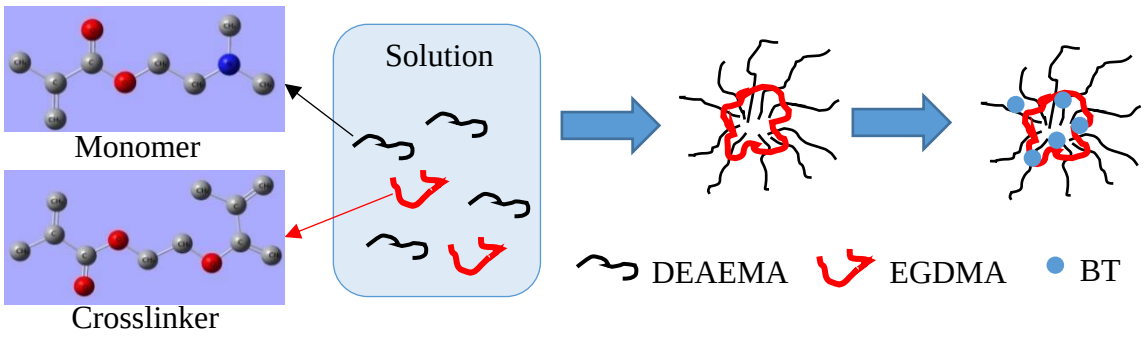

Figure 1. Schematic of the synthesis of the intelligent corrosion inhibitor.

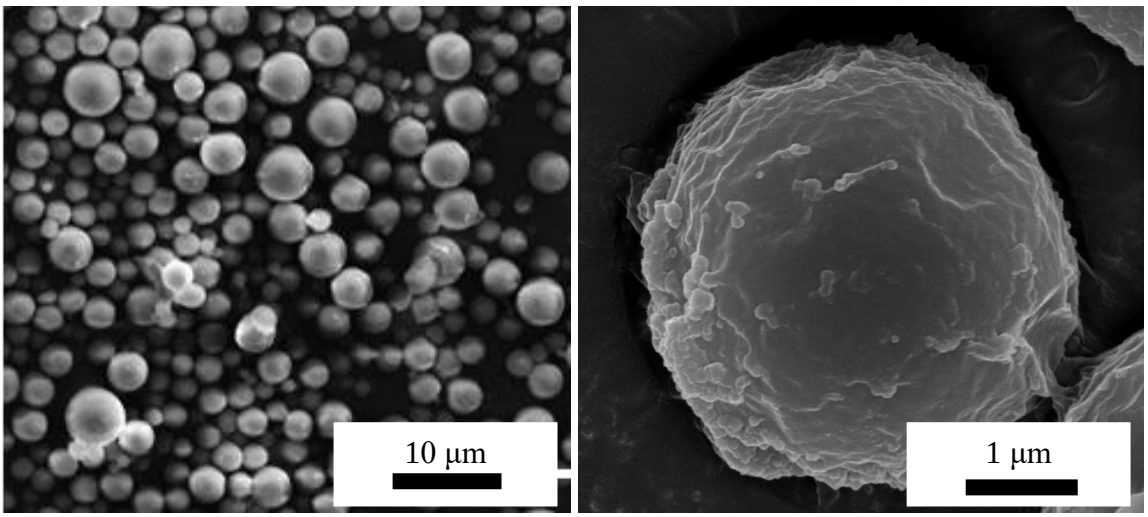

Figure 2. SEM profiles of the PDEAEMA microspheres in different magnification.

3.2 pH response of the PDEAEMA microspheres

The shrinkage or swelling behaviors of the PDEAEMA microspheres in various buffer solutions (pH 2.0, pH 6.0, pH 9.0) were observed using an optical microscope, as shown in Fig. 3. The microspheres were dyed with Coomassie brilliant blue for more effective observations. When the pH was 9.0 in the alkaline environment, the diameter of the PDEAEMA microspheres was approximately 3 μm. The microspheres swelled from 3 μm to 10 μm in the acidic environment. There was an obvious three-fold increase in the diameter found by adjusting the pH value from 9.0 to 2.0. Thus, PDEAEMA microspheres are promising carriers of intelligent corrosion inhibitors because of their good pH sensitivity [17].

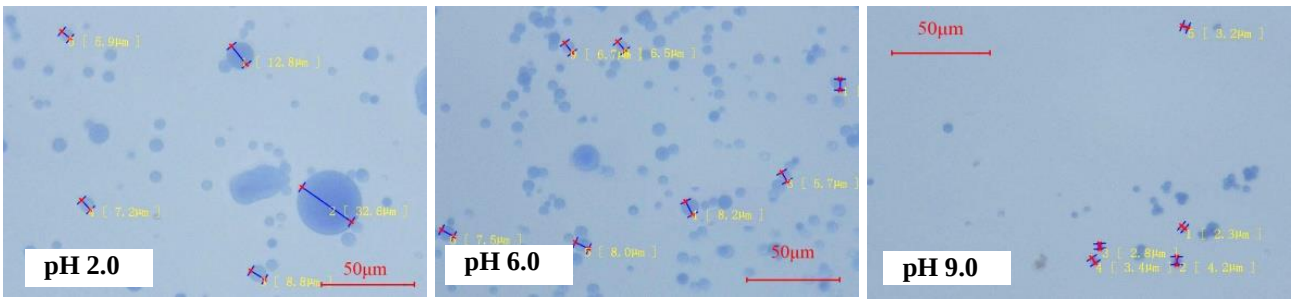

Figure 3. Optical micrographs of the PDEAEMA microspheres at different pH values.

The superior pH sensitivity of the PDEAEMA microspheres is mainly attributed to the deprotonation of the tertiary amine groups (-$(CH_3CH_2)_3N$). At low pH values (high H^+ concentration), the tertiary amines of the PDEAEMA microspheres are protonated, and the microspheres swell due to the strong charge repulsion between the positive ions. As a result, BTA was easily released from the PDEAEMA network structure in acidic environments (see Fig. 4). In Wang's work, PDEAEMA was proposed to be used with hydrophilic poly(ethylene gly-col) (PEG) as the macroinitiator for tumour-targeted drug delivery [18].

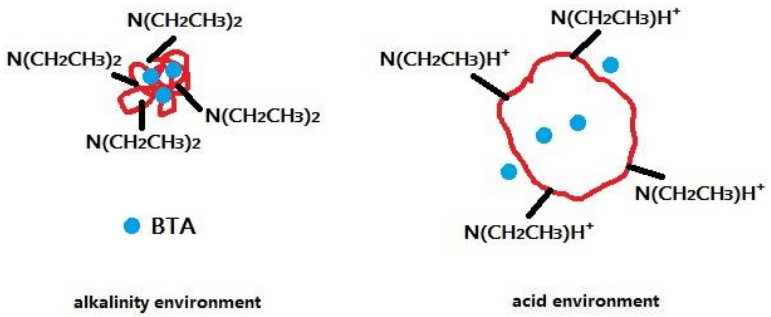

Figure 4. Swelling of the PDEAEMA microspheres and release of BTA inhibitor.

3.3 BTA content of the intelligent inhibitor

The PDEAEMA microspheres were immersed in the BTA-ethanol solution to prepare the intelligent corrosion inhibitor. The amount of entrapped BTA was determined from the difference between the concentration of BTA in the initial and final BTA solutions. The UV absorption spectra of the BTA solutions are showed in Fig. 5. The average amount of the BTA loaded into the PDEAEMA microspheres was approximately 1.5 wt%, which is similar to that in the previous study [19].

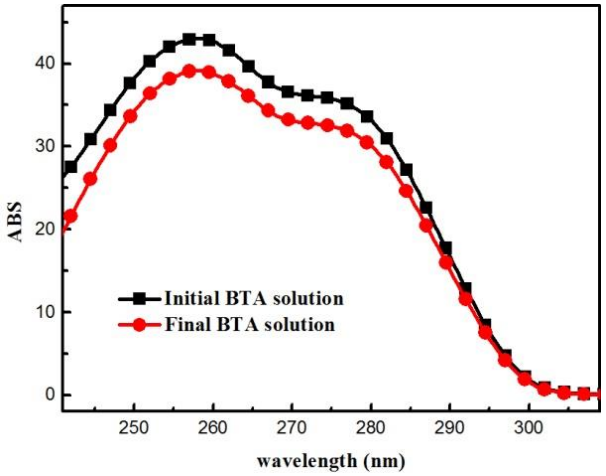

Figure 5. Absorbance curves of the BTA solution before and after the immersion of PDEAEMA microspheres.

3.4 Controlled release of BTA from the intelligent inhibitor

The BTA release profiles of the intelligent corrosion inhibitor in different pH solutions (pH 2.0, 6.0, and 9.0) are shown in Fig. 6. In the first 1.5 h, there was approximately 70%, 50%, and 30% release of BTA at pH 2.0, 6.0, and 9.0, respectively. After 6 h, the release of BTA at pH 2.0 was almost complete, whereas at pH 9.0 after 15 h, the BTA release was only 60%. These results confirm that the release rate of BTA from the intelligent inhibitor strongly depends on the pH value, which is consistent with the swelling behavior of the PDEAEMA microspheres in Fig. 3. As discussed above, this is attributed to the larger microsphere size and easier diffusion of BTA with decreasing pH.

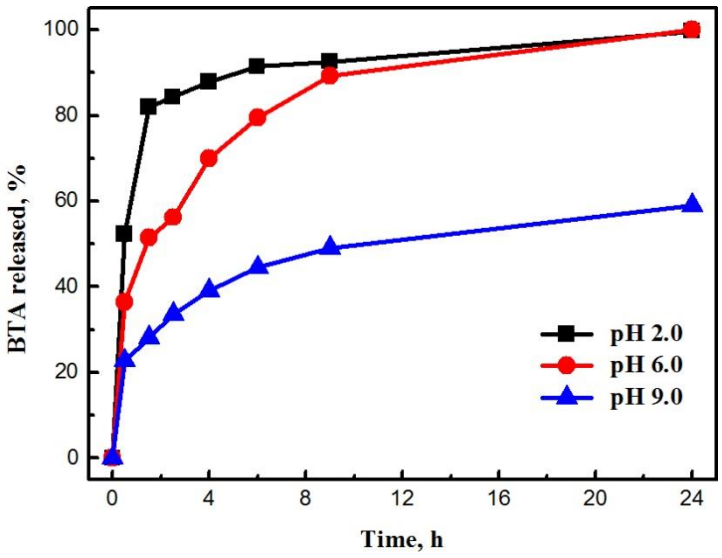

Figure 6. Release profile of BTA from the intelligent corrosion inhibitor at different pH values.

3.5 Corrosion inhibition efficiency of the intelligent inhibitor

The potentiodynamic polarization curves and electrochemical impendence spectra of the carbon steel after immersion in the NaCl solution at pH 6.0 for 6 h are shown in Fig. 7. The fitting data of the electrochemical curves were calculated to quantify the corrosion inhibition properties of the intelligent corrosion inhibitor as listed in Table 1.

The three polarization curves showed similar shapes with no obvious passivation zone and similar corrosion potentials of -840 mV_{SCE}. There was no significant difference in the anodic and cathodic polarizability as well. However, both the anodic and cathodic currents were reduced after the addition of the intelligent corrosion inhibitor. The corrosion current densities were 0.78, 0.58, and 0.22 $\mu A/cm^2$, in the solutions without BTA, with BTA, and with intelligent corrosion inhibitor, respectively. This indicates that the intelligent corrosion inhibitor can suppress both the anodic and cathodic reactions on the steel surface. And the inhibition efficiency was 70% for the intelligent corrosion inhibitor with a dose of 0.25 g/L.

The three impedance spectra with one time constant were described with an R(QR) equivalent electrical circuit, in which R_s is solution resistance, R_p is polarization resistance, and CPE is constant phase element. The R_p I n the case of the intelligent corrosion inhibitor was 1.7 times greater than that in the blank solution, and the CPE was much lower. The comparison results in Table 1 suggest that the use of intelligent corrosion inhibitor promotes the formation of a stable barrier film on the steel surface and inhibits metal dissolution in the electrolyte.

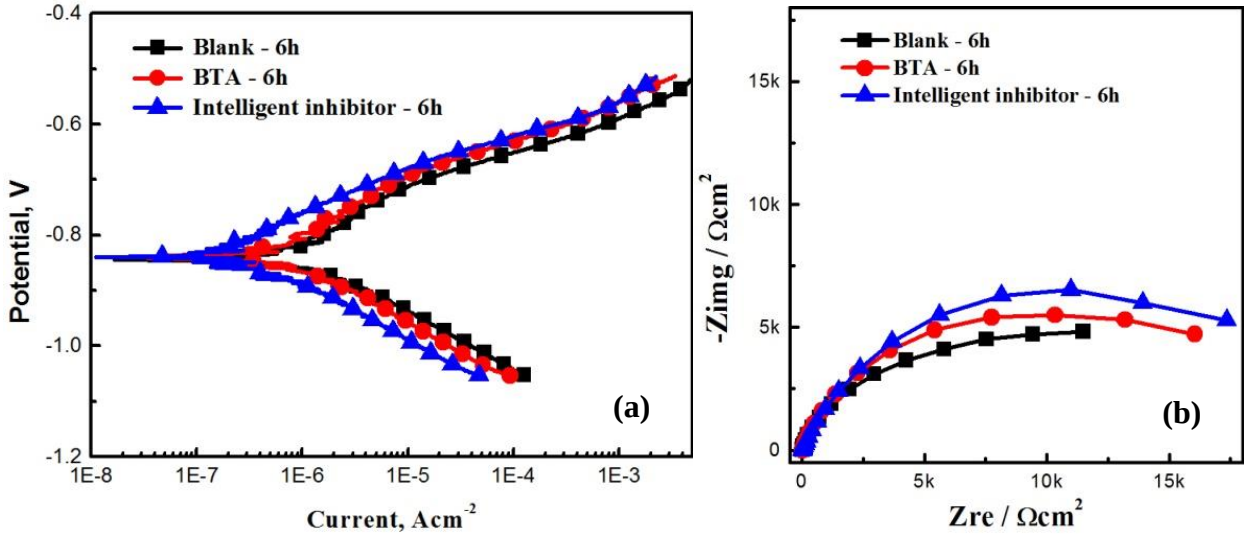

Figure 7. Potentiodynamic polarization curves (a) and electrochemical impendence spectra (b) for the carbon steel after immersion in the NaCl solution at pH 6.0 for 6h.

Table 1. Fitting data for the polarization curves and electrochemical impendence spectra.

Environment	Blank	BTA inhibitor	intelligent inhibitor
Total BTA, mg/L	0	25	25
E_{corr}, mV_{SCE}	-848	-843	-838
I_{corr}, $\mu A/cm^2$	0.782	0.582	0.216
R_s, Ωcm^2	16.78	14.48	15.15
R_p, Ωcm^2	1.07E4	1.45E4	1.80E4
CPE, $\Omega^{-1}cm^{-2}s^n$	1.67E-4	1.38E-4	1.06E-4
n-CPE, s^{-n}	0.82	0.81	0.77

4. CONCLUSIONS

An intelligent corrosion inhibitor exhibiting low-pH-triggered corrosion protection in an environment with variable pH is developed based on oil-in-water emulsion synthetic PDEAEMA microspheres. The average particle size of the microspheres is 3 μm. At acidic pH conditions, the protonated diethyl amino groups cause electrostatic repulsion. Therefore, the microspheres exhibit a significant increase in the swelling, i.e., at pH 2.0, the average particle size of the microspheres is approximately 10 μm. The intelligent corrosion inhibitor based on the pH-sensitive microspheres suggests pH-dependent release of the BTA corrosion inhibitor. From the electrochemical results, the intelligent corrosion inhibitor has long-term and efficient corrosion inhibition performance owing to the pH-dependent supply of BTA.

ACKNOWLEDGMENTS
This work was supported by the training program of scientific and technological innovation for undergraduates, Guangdong, China (No. pdjh2019b0231).

References

1. X.G. Li, D.W. Zhang, Z.Y. Liu, C.W. Du, C.F. Dong, *Materials science: Share corrosion data, Nature*, 527 (2015) 441.
2. E. Abdullayev, R. Price, D. Shchukin, Y. Lvov, *ACS applied materials and interfaces*, 1 (2009) 1437.
3. J.L. Yao, B. Ren, Z.F. Huang, P.G. Cao, R.A. Gu, Z.Q. Tian, *Electrochimica Acta*, 48 (2003) 1263.
4. M.M. Mennucci, E.P. Banczek, P.R.P. Rodrigues, I. Costa, *Cement and Concrete Composites*, 31 (2009) 418.
5. P.P. Ren, D.W. Zhang, C.F. Dong, X.G. Li, *Materials Letters*, 160 (2015) 480.
6. A.A. Javidparvara, R. Naderia, B. Ramezanzadehb, G. Bahlakeh, *Journal of Industrial and Engineering Chemistry*, 72 (2019) 196.
7. T. Matsuda, K.B. Kashi, K. Fushimi, V.J. Gelling, *Corroion Science*, 148 (2019) 188.
8. Y.W. Tian, C.F. Dong, G. Wang, X.Q. Cheng, X.G. Li, *Materials Letters*, 236 (2019) 517.
9. K.A. Yasakau, A. Kuznetsova, S. Kallip, M. Starykevich, J. Tedim, M.G.S. Ferreira, M.L. Zheludkevich, *Corrosion Science*, 143 (2018) 299.
10. J. Hu, S.S. Feng, W. Abas, B. Pingguan-Murphy, F. Xu, *Biosensors and Bioelectronics*, 79 (2016) 98.
11. E.V. Skorb, A.G. Skirtach, D.V. Sviridov, *Acs Nano*, 3 (2009) 1753.
12. J. Lu, J. Wu, J. Chen, Y.L. Jin, T. Hu, K.B. Walters, S.J. Ding, *Journal of Applied Polymer Science*, 132 (2015) 42179.
13. D. Dupin, S. Fujii, S.P. Armes, O. Reeve, S.M. Bavter, *Langmuir*, 22 (2006) 3381.
14. A. Latnikova, D. Grigoriev, M. Schenderlein, H. Moehwald, *Soft Matte*r, 8 (2012) 10837.
15. Q. Zheng, T. Lin, H. Wu, L. Guo, P.R.Ye, Y.L. Hao, Q.Q. Guo, J.Z. Jiang, F.F. Fu, G.N. Chen, *International journal of pharmaceutics*, 463 (2014) 22.
16. A. Kondo, H. Fukuda, *Colloids and Surfaces A: Physicochemical and Engineering Aspects*, 153 (1999) 435.
17. C.M. González-Henríquez, P.A. Alfaro-Cerda, D.F. Veliz-Silva, M.A. Sarabia-Vallejos, C.A. Terraza, J. Rodriguez-Hernandez, *Applied Surface Science*, 457 (2018) 902.
18. G.Y. Wang, L.M. Zhang, *Reactive and Functional Polymers*, 107 (2016) 1.
19. M. Saremi, M. Yeganeh, *Corrosion Science*, 86 (2014) 159.